Acta Neuropathol (2001) 101 : 129–139
DOI 10.1007/s004010000275

REGULAR PAPER

Angelika F. Hahn · Peter J. Ainsworth
Charles F. Bolton · Juan M. Bilbao
Jean-Michel Vallat

Pathological findings in the x-linked form of Charcot-Marie-Tooth disease: a morphometric and ultrastructural analysis

Received: 11 April 2000 / Revised, accepted: 16 June 2000 / Published online: 21 October 2000

Abstract Mutations in the connexin 32 gene (*Cx 32*) are associated with the x-linked form of Charcot-Marie-Tooth disease (CMTX) and segregate with a CMT 1 phenotype. The gap junction protein Cx 32 is expressed in myelinating Schwann cells and has been localized to regions of non-compacted cytoplasm in paranodes and in Schmidt-Lanterman incisures. Mutant Cx 32 myelin proteins are predicted to impair Schwann cell functions. We have studied the resulting pathology in motor and sensory nerves from the probands of 13 CMTX kindreds with precisely defined genotype. This report provides a detailed descriptive and morphometric analysis of 14 CMTX nerve biopsy samples, taken at various stages in the development of the neuropathy and studied by light and electron microscopic examination. Findings indicated unusually prominent changes in paranodal myelin with resulting widened nodes of Ranvier, but with segmental demyelination being less common. In parallel early axonal cytoskeletal abnormalities were noted, which were followed later by axonal atrophy, degeneration and loss of myelinated nerve fibers, occurring in a length-dependent fashion. Regenerative sprouting was also unusually prominent. Ultrastructural abnormalities included a frequent dilatation of the adaxonal spaces, prominence of the adaxonal Schwann cell cytoplasm and widening of the Schmidt-Lanterman incisures. We conclude that mutations in Cx 32 gap junction protein lead to a compromise of Schwann cell functions and to impaired Schwann cell-axon interactions with subsequent pathology in both myelin and axons.

Keywords Charcot-Marie Tooth disease · CMTX · Connexin 32 · Nerve biopsy · Ultrastructure

A. F. Hahn (✉) · C. F. Bolton
Department of Clinical Neurological Sciences,
The University of Western Ontario,
London Health Sciences Centre, 339 Windermere Road,
London, Ontario, Canada
e-mail: angelika.hahn@lhsc.on.ca

P. J. Ainsworth
Department of Biochemistry, The University of Western Ontario,
London Health Sciences Centre, London, Ontario,
Canada N6A 5A5

J. M. Bilbao
Department of Pathology, The University of Toronto,
St. Michael's Hospital, Toronto, Ontario, Canada

J.-M. Vallat
Department of Neurology, University of Limoges, Limoges,
France

Introduction

Charcot-Marie-Tooth disease (CMT) represents a heterogeneous group of inherited neuropathies that share a characteristic clinical phenotype and chronic progressive course [12, 18]. Two major categories have been distinguished based on electrophysiological and pathological findings: CMT type 1 (demyelinating variant) and CMT type 2 (axonal variant). Recent discoveries of the causative molecular genetic defects have allowed a more precise classification [25]. However, careful genotype/phenotype correlations have revealed a far greater complexity, in that the phenotypic manifestations may be determined not only by the deleterious effects of the mutated gene but also by modifying genetic and environmental factors [6, 26, 39, 42].

Mutations in three genes coding for the myelin proteins: peripheral myelin protein 22 (PMP22), myelin protein zero (MPZ), and for connexin 32 (Cx 32) segregate with a CMT 1 phenotype. The association of mutations within the coding region of *Cx 32* and the x-linked form of CMT (CMTX) was demonstrated first in 1993 by Bergoffen et al. [4]. Since then, approximately 160 distinct CMTX-causing mutations have been described, the majority of which are missense mutations spread throughout the open reading frame of *Cx 32* [25]. Less usual observations included the deletion of the entire *Cx 32* gene coding sequence [1] and two instances of non-coding regulatory region mutations [19]. *Cx 32* gene mutations resulted in a consistent clinical phenotype with pes cavus, atrophy of the distal leg muscles and of the intrinsic hand muscles, as

well as distal sensory loss [16]. Nerve conduction velocities were slowed to an intermediate range and our studies indicated, in general, uniform slowing of conduction, with involvement of both motor and sensory fibers [16, 17, 27]. Occasional observations of non-uniform conduction slowing in a few severely affected patients have also been reported [15, 41]. Recorded amplitudes of compound muscle action potentials (CMAPs) and evoked sensory nerve action potentials (SNAPs) were markedly reduced; together these findings were consistent with combined paranodal and segmental demyelination and chronic, distal axonal degeneration.

To date, there have been few systematic analyses of nerve biopsy material [16, 35, 39]. Very brief descriptions of the pathology were contained in reports of single families or small series [5, 23, 33, 38, 41] and the pathological alterations have been variably interpreted as a primarily axonal versus a primarily demyelinating process.

The gap junction protein Cx 32 is intrinsically expressed in myelinating Schwann cells and has been localized to regions of non-compacted cytoplasm in paranodes and incisures [36]. Cx 32 gap junctions are presumed to form functional radial diffusion pathways between the outer and the adaxonal Schwann cell cytoplasm [3]. Mutant Cx 32 proteins are thus predicted to impair Schwann cell functions, which undoubtedly will also affect the intricate cell-cell relationship of the Schwann cell and its associated axon. Thus, the detailed examination of the human pathology will provide an opportunity to study the biological effects of a known molecular Schwann cell defect.

This report concerns a detailed descriptive and morphometric analysis of 14 CMTX nerve biopsy specimens studied by both light and electron microscopic examination.

Patients and methods

Patients

The index cases of 14 families with genetically confirmed CMTX were studied. Diagnostic biopsy samples of peripheral nerve (the superficial and deep peroneal or sural nerves at the level of the lateral malleolus and/or the radial dorsal cutaneous nerve at the wrist), as well as muscle (anterior tibialis or peroneus brevis) at ages ranging from 13 to 71 years were investigated. In family I, biopsy specimens from two affected males, ages 16 and 61 years, were available, allowing an assessment of the evolution of the nerve pathology. All patients had been studied on one or more occasions by detailed electrophysiological examinations. In each of the probands, the precise mutation in the coding region of the *Cx 32* gene had been identified by genomic DNA analysis.

Histological techniques

Nerve biopsy samples were fixed in 2.5% phosphate-buffered glutaraldehyde at 4°C for 4 h; they were divided in two to three portions, each about 1 cm in length, and processed according to standard techniques for light and electron microscopy and teased fiber preparation [9]. Toluidine blue-stained semithin sections (0.5–1 μm) were prepared for light microscopy. Ultrathin sections were double-stained with uranyl acetate and lead citrate and examined with a Philips electron microscope. Muscle biopsy tissues were divided in three parts and processed as follows: frozen sections; Zenker's fixed, paraffin-embedded sections; and 2.5% buffered glutaraldehyde-fixed/resin-embedded semithin sections. Frozen sections were stained with hematoxylin and eosin, Gomori trichrome, DPNH, ATPase (at pH 4.2, 4.6, 9.8) and PAS reagents and were viewed with the light microscope. Semithin sections were stained with toluidine-blue and selected areas of these were prepared for viewing under the electron microscope.

Quantitative morphological studies

For teased fiber preparations, a minimum of 100 myelinated fibers of each nerve were isolated, transferred and aligned on ten glass slides and graded according to Dyck et al. [9]. Morphometric analysis of myelinated fibers was performed using a Zeiss videoplan. The fiber density was expressed as number of fibers/mm^2 of endoneurial area and a histogram of myelinated fibers was plotted. The density of unmyelinated fibers was determined from serial electron micrographs (16 exposures per nerve at 3,000 magnification) and expressed as numbers of unmyelinated fibers/mm^2 endoneurial area.

To determine the axon diameter/fiber diameter ratio, the fiber diameter and axonal diameter were measured with a millimeter rule in a minimum of 35 randomly chosen myelinated nerve fibers for each nerve. A mean G/ratio (axonal diameter/fiber diameter) was calculated of all fibers measured.

A cluster formation was defined as a group of two or more myelinated fibers limited by an original Schwann cell basal lamina.

Electrophysiological techniques

Neurophysiological studies were performed as described previously [16, 17, 41].

Molecular genetic studies

Methods used to identify and characterize the *Cx 32* mutations have been described previously [1, 17, 21]. In total, 18 kindred with CMTX were identified by genomic DNA analysis. The *Cx 32* mutations were spread throughout the coding region and included 13 missense mutations, 4 stop codon mutations, and in 1 family, a deletion mutation that eliminated the entire coding sequence of *Cx 32*.

Results

Molecular genetic and clinical findings

We studied 18 families with defined CMTX genotype. Table 1 lists the identified mutations in the coding region of the *Cx 32* gene. These included: 11 different (13 in total) missense mutations, predicting non-conservative amino acid substitutions, spread throughout the various domains of the Cx 32 protein (two families each shared a serine to leucine substitution at codon 26, and a further two families a glutamine to lysine substitution at codon 208). In addition, one 8-bp deletion/4-bp insertion frame-shifting mutation and three nonsense mutations were encountered, all four predicting premature termination of protein translation and likely loss of Cx 32 function. A further unique mutation with a greater than 850-bp deletion was characterized that eliminated the entire coding sequence of the

Table 1 Summary of the 18 families studied with defined CMTX genotype, showing the identified mutations in the coding region of the *Cx 32* gene (*n* nerve, *peron.* superficial and deep peroneal nerve, *radial* dorsal cutaneous nerve, *TA* tibialis anterius muscle)

Family/no. affected[a]	Mutation	Substitution	Amino acid no.	Cx 32 domain	Range of phenotype in males	Onset of symptoms	Additional signs/ symptoms	Pathology examined
X/12	G→A	Arg→Gln	15	N-terminal	Moderate to severe	1st decade	Scoliosis, tremor	sural n.
V/3	C→T	Ser→Leu	26	1st transmembrane	Severe	1st decade	–	peron. n/TA
XIV/3	C→T	Ser→Leu	26	1st transmembrane	Severe	1st decade	Pain	peron. n.
II/9	T→C	Met→Thr	34	1st transmembrane	Moderate to severe	1st decade	Scoliosis, pain	sural n.
XV	C→T	Thr→lle	55	1st extracellular loop				
III/I	G→A	Arg→Gln	75	2nd transmembrane	Moderate	–	–	–
XVI/80	C→T	Pro→Leu	87		Severe	1st decade		radial n.
VII/7	G→A	Val→Met	95	Intracellular loop	Moderate	2nd decade	Pain	TA muscle
XVII/I[b]	G→T	Glu→stop	102	Intracellular loop	?	2nd decade	–	sural n.
IV/6	C→T	Arg→Trp	107	Intracellular loop	Moderate	2nd decade	–	–
VIII/6	8-bp del/ 4-bp insert	Premature stop	119	Intracellular loop	Moderate to severe	1st decade	–	TA muscle
XIII/I[c]	G→A	Val→Met	139	3rd transmembrane	?	–	–	sural n.
XVIII/3	C→T	Arg→Cyst	183	2nd extracellular loop	Severe	1st decade	–	peron. n. & muscle
VI/4	G→A	Glu→Lys	208	C-terminal	Severe	1st decade	Scoliosis	peron. n.
IX/3	G→A	Glu→Lys	208	C-terminal	Severe	1st decade	–	sural n./TA
1/45[d]	C→A	Tyr→stop	211	C-terminal	Severe	1st decade	Scoliosis, pain	peron. n./TA
XI/15	T→A	Cys→stop	217	C-terminal	Moderate to severe	1st decade	–	–
XII/4	Deletion of entire coding sequence			All	Severe	1st decade	–	peron. n./TA

[a]No. of affected individuals assessed by detailed neurological examination
[b][41]
[c]Small pedigree; proband heterozygous female
[c][16]

Cx 32 gene, predicting in affected males an absence of *Cx 32* gene product and, thus unquestionably loss of Cx 32 gap junction function. The consequences of this mutation in affected males might be expected to be not unlike those observed in *Cx 32* knockout mouse mutants that have been created by a targeted disruption of the *Cx 32* gene [37].

These various *Cx 32* gene mutations segregated with the typical CMTX phenotype, which we have described previously [16], and which is characterized by pes cavus, atrophy of distal leg muscles and intrinsic hand muscles and sensory abnormalities; findings of a length-related motor and sensory neuropathy that progresses with age. Affected males who were hemizygous for the mutations described were more severely affected, showing onset of symptoms in early childhood, while affected and heterozygous females commonly had only mild clinical signs. Only approximately 10% of female carriers showed a moderately severe clinical phenotype with the usual onset of symptoms in the second to third decade. Nonetheless, in this study six index cases and nerve biopsy specimens were from women, who most often belonged to small families and had no knowledge of affected relatives or else who had come to biopsy prior to the identification of the gene mutation.

Pathological observations

Surgical biopsy samples were taken from either the sural nerve (n=6), the superficial and deep peroneal nerves (n=7), or the dorsal cutaneous radial nerve (n=1), as well as from the tibialis anterior and peroneus brevis muscles (n=8). In all, peripheral nerve tissues from eight hemizygous male individuals (ages ranging from 13 to 66 years) and from six heterozygous female gene carriers (ages 30 to 71 years) were examined by light and electron microscopy and by teased fiber analysis. In two patients only muscle tissues were examined.

Morphological observations

The light microscope finding that were typical of CMTX are illustrated in the sural nerve biopsy specimen of a 13-year-old boy (Fig. 1A) and in that of a 45-year-old man (Fig. 1B), respectively, both of whom harbor the same missense mutation at codon 208. In the biopsy specimen from the younger individual (Fig. 1A), there was only a mild reduction in myelinated fibers noted (density 7,042/mm^2; control 9,300/mm^2); the myelin sheath thickness of most fibers was fairly normal (G/ratio 0.54±0.09;

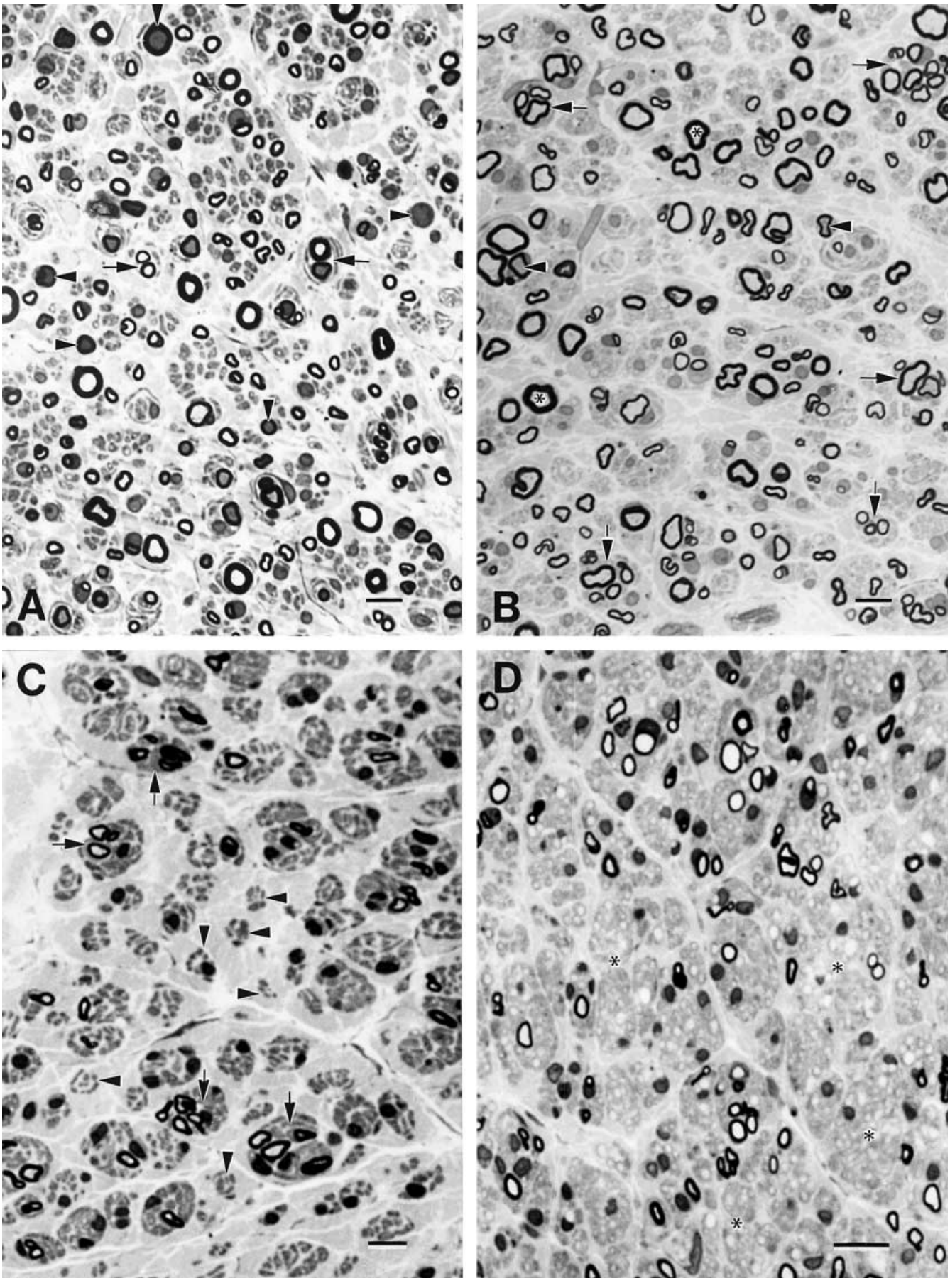
A
B
C
D

control 0.52±0.08). The presence of numerous clusters of regenerating myelinated nerve fibers, each ensheathed by disproportionately thin myelin, as well as numerous darkly stained axons (arrowhead) was demonstrated. Ultrastructurally, these corresponded to changes in the axonal cytoskeleton, with a condensation and increase of neurofilaments, and a relative decrease of microtubules (Fig. 2). A section from a biopsy specimen, obtained from an older individual carrying the same mutation, is illustrated in Fig. 1B. The density of myelinated fibers in this biopsy was more noticeably reduced (5,925/mm^2; control 9,300/mm^2), and relatively few fibers showed a normal myelin sheath thickness (asterisk); the majority of fibers were surrounded by relatively thin myelin (G/ratio 0.7±0.09) and many myelinated fibers were aggregated in clusters (arrows), indicating attempts of regeneration. Axoplasmic condensations were much less common (arrowhead). Histopathological changes, observed in the sural nerve biopsy of a 32-year-old heterozygous female patient with a moderately severe clinical phenotype, were qualitatively similar, but less prominent. Again, fibers were relatively thinly myelinated and some were arranged in clusters (G/ratio 0.65±0.09); a few fibers were surrounded by supernumerary Schwann cell processes, in keeping with small onion bulb formations. Of particular interest were observations made in the biopsy samples of the deep peroneal nerve (DPN) and the superficial peroneal nerve (SPN), derived from a 66-year-old male patient who harbored a deletion mutation of the entire coding region of the *Cx 32* gene, with a documented complete absence of the *Cx 32* gene product. The DPN motor nerve biopsy specimen (Fig. 1C) showed severe loss of myelinated nerve fibers (density 2,250/mm^2; control 7,450/mm^2), as well as numerous plates of denervated Schwann cells (arrowhead) and ample deposition of collagen; clusters of residual regenerated nerve fibers were also noted (arrows). These findings corresponded with observations of severe and chronic denervation atrophy in biopsy specimens of distal leg muscles. The cutaneous sensory nerve (SPN) of the same individual (Fig. 1D) showed much less prominent loss of myelinated fibers (density 8,625/mm^2; control 9,300/mm^2), which was due, at least in part, to a very unusual prominence of proliferated axons. These were either invested by thin myelin sheaths, or not myelinated and were associated with redundant Schwann cell material (unmyelinated fiber density 35,800/mm^2; control 29,000/mm^2). The unusual proliferation or aggregation of small axons was better appreciated in electron micrographs obtained from this nerve (Fig. 3).

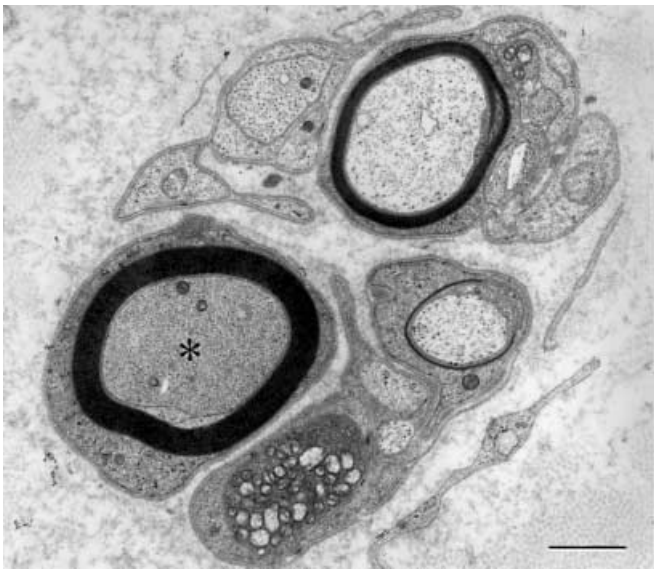

Fig. 2 Electron micrograph of biopsy sample shown in Fig. 1A. Cluster of myelinated nerve fibers. Note the axonal cytoskeletal changes with marked increase in number and density of neurofilaments and decrease in microtubules (*asterisk*). *Bar* 1 μm

Electron microscope examination of CMTX biopsy material from all disease stages revealed a number of remarkable ultrastructural findings. Myelinated nerve axons were often surrounded by unusually prominent collars of adaxonal Schwann cell cytoplasm and complex arrangements of the inner mesaxons (Fig. 4), and Schmidt-Lanterman incisures appeared widened (regions in which myelin is non-compacted and in which the Cx 32 gap junction protein is selectively expressed). Moreover, in many myelinated fibers a separation of the myelin sheath from the axon was observed, creating a clear space that appeared either empty or contained vesicular material (Fig. 5). Such changes could be discerned easily with both the light and electron microscope; they were observed in well-fixed biopsies that showed no handling artifacts, and were present in all of the examined CMTX nerves. Therefore, they appear to be genuine and specific for this variant form of CMT. It is possible that such peri-axonal clear spaces observed in cross-sections of nerve corresponded to alterations within the non-compacted Schwann cell cytoplasm of paranodal myelin loops noted in longitudinally oriented nerve fibers (Fig. 6C). Such changes in paranodal myelin attachments, as well as an apparent widening of the nodal gap, were unusually frequent in these biopsy specimens and could easily be recognized in longitudinally oriented

◀ **Fig. 1** **A** Sural nerve biopsy sample from a 13-year-old male bearing a mutation at codon 208. The density of myelinated fibers is only slightly reduced; clusters of regenerating fibers are indicated by *arrows*; numerous axons appear darkly stained (*arrowheads*), which corresponds with cytoskeletal alterations noted by electron microscopy. **B** Sural nerve biopsy sample from a 45-year-old male bearing the same mutation at codon 208. Myelinated fibers are reduced in number and only few fibers show a normal myelin sheath thickness (*asterisk*). Clusters of regenerating and thinly myelinated fibers are very prominent (examples indicated by *arrows*). Fewer axons are darkly stained (*arrowhead*). **C** Deep peroneal nerve biopsy sample (motor nerve) from a 66-year-old male with a >850-bp deletion of the entire coding sequence of *Cx 32*. Note the severe loss of myelinated fibers resulting in numerous plates of denervated Schwann cells (*arrowhead*) and increase in collagen; clusters of myelinated fibers are present (indicated by *arrow*). **D** Superficial peroneal nerve biopsy sample (cutaneous sensory nerve): myelinated fibers are reduced in number and residual fibers have proportionately thin myelin sheaths. Note the unusual prominence of proliferated nerve axons throughout the biopsy specimen (*asterisks*). **A–D** Toluidine blue-stained 1-μm transverse sections, *bars* 10 μm

Fig. 3 Electron micrograph derived from superficial peroneal nerve biopsy sample illustrated in Fig. 1D. Note the unusually prominent number of small axons (*asterisks*) that are surrounded by ample Schwann cell cytoplasm and probably reflect axonal sprouting. *Bar* 1 μm

nerve sections (Fig. 6B) and in teased nerve fibers. By light microscopy, they appeared either as long demyelinated segments that were associated with intercalated supernumerary Schwann cells, or as widened nodes of Ranvier (Fig. 6A).

Teased fiber preparations

The most remarkable findings from the study of teased fibers were the unusually high incidence of widened nodes of Ranvier that were observed in association with an apparent remodeling of the paranodal myelin attachments (categorized as C fibers, according to Dyck et al. [9]). In contrast, segmental demyelination or remyelination was much less frequent (categories D and F). Moreover, there was little evidence of actively ongoing axonal degeneration (category E). The data are summarized in Table 2.

Morphometry

Representative histograms of myelinated and unmyelinated nerve fibers in the biopsy specimens from the superficial peroneal nerves of a 16-year-old and a 61-year-old male patient of family I have been published previously [16]. We noted a loss of large myelinated fibers that increased with the patients' age and with the progression of the neuropathy. The fiber histograms were shifted towards smaller fibers, in keeping with the observed abundance of clusters of thinly myelinated fibers.

The morphometric data from all 14 nerve biopsy samples are listed in Table 2. They demonstrate a moderate re-

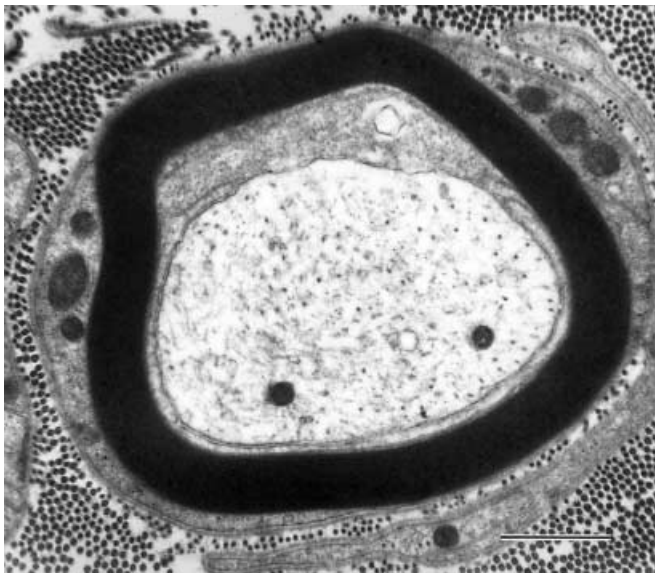

Fig. 4 Electron micrograph. Representative illustration of the unusually wide collar of adaxonal Schwann cell cytoplasm and complex arrangements of the inner mesaxon observed in many fibers. *Bar* 1 μm

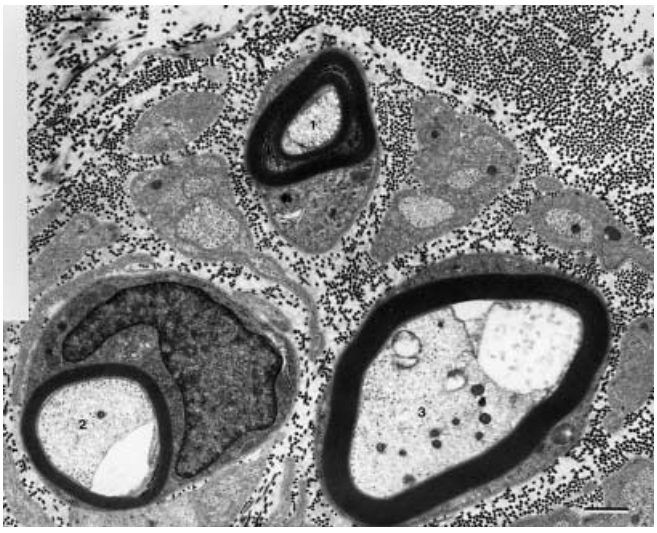

Fig. 5 Electron micrograph. Representative illustration of the frequently observed separation of the axons from their associated myelin sheaths, creating a space which either appeared empty or was filled with vesicular debris (*asterisks* in fibers 2 and 3). *Bar* 1 μm

duction in the density of myelinated fibers in the cutaneous sensory nerve specimens and severe axonal loss in the examined motor nerves. The myelinated nerve fiber histograms were skewed towards smaller and more thinly myelinated fibers, a finding also expressed in the altered relationship of axon diameter/fiber diameter, e.g., an elevated mean G/ratio.

Muscle biopsies

Biopsy samples from distal leg muscles were available for study by light and electron microscopy from eight of the affected individuals. The histological findings corresponded to large grouped muscle fiber atrophy, indicative of chronic partial denervation and reinnervation of muscle. Several specimens contained small intramuscular nerve twigs composed of thinly myelinated nerve fibers, probably representing mainly residual afferent sensory nerve fibers.

Discussion

Pathological observations in this large number of CMTX biopsy specimens, taken at various time points in the evolution of the neuropathy, indicate three main and seemingly characteristic features: (1) unusually frequent alterations of paranodal myelin, (2) unusually prominent clusters of regenerating thinly myelinated nerve fibers, and (3) progressive loss of large myelinated nerve fibers.

These changes were consistently present and could easily be discerned with the light microscope in resin-embedded biopsy material. Paranodal myelin changes were best appreciated, however, in teased nerve fibers or in longitudinally oriented nerves using electron microscopy. The prevalence of an apparent widening of the nodes of Ranvier, due to the alteration and the remodeling of paranodal myelin attachments, was intriguing, all the more since it was not observed to be accompanied by a similar frequency of segmental demyelination and remyelination, as is usually the case in the acquired demyelinating neuropathies. Therefore, these changes in paranodal myelin may be specific for CMTX and may be especially significant because they coincide with the localization of the Cx 32 protein to the paranodal region [36]. Conceivably, they could represent a primary abnormality of the Schwann cell, arising from the molecular genetic defect in the Cx 32 gap junction protein and would be expected to alter the physiological properties of nerve fibers. Comprehensive electrophysiological studies in our laboratories in 82 affected persons and 33 at risk family members indicated, in general, a uniform slowing of conductions along the length of the nerves consistent with demyelination of motor and sensory fibers [16, 17]. Others have emphasized the observations of non-uniform conduction slowing in a few severely affected patients [15, 41]. These results correlate with the present morphological observations and the variations due to gender and age.

Previous pathological reports, including our own, have emphasized the very obvious finding of axonal degeneration and loss of motor and sensory nerve fibers [5, 16, 31, 38]. This occurs in a length-dependent fashion and correlates well with the distally accentuated atrophy of leg muscles and of intrinsic hand muscles. Pes cavus foot deformity, due to atrophy of small foot muscles, and wasting of the thenar muscles in the hand are present very early on, and are a characteristic feature of this CMT variant. Careful electrophysiological examinations have demon-

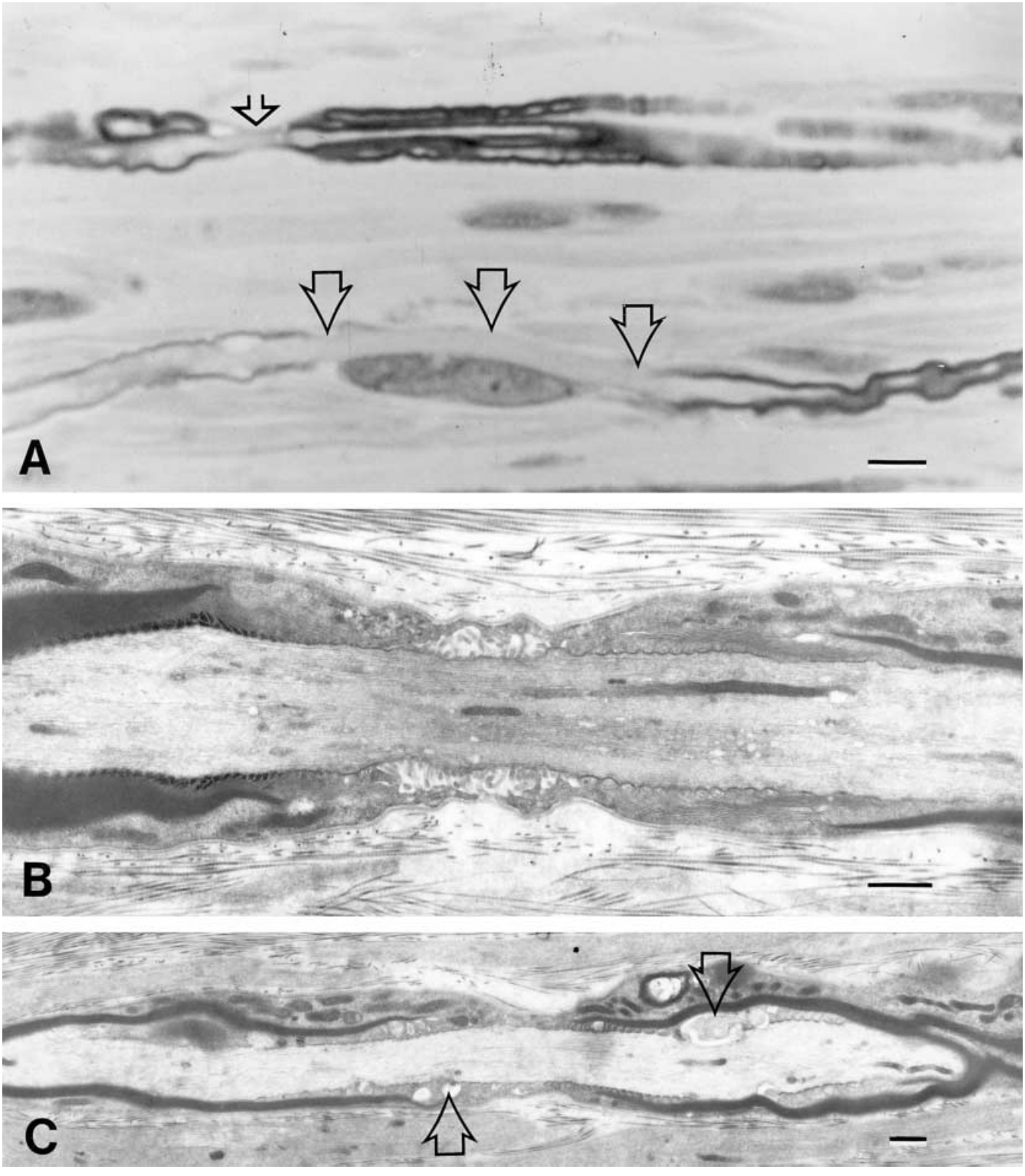

Fig. 6 **A** Superficial peroneal nerve. Representative illustration of frequent paranodal changes. Nodes of Ranvier appear widened (*upper arrow*); or paranodal demyelination was more extensive, with longer demyelinated segments that were associated with supernumerary Schwann cells (delineated by *lower arrows*) ; toluidine blue-stained, 1-μm longitudinal nerve section. **B,C** Electron micrographs of longitudinally oriented nerve fiber. **B** Representative illustration of abnormal paranodal myelin attachments. **C** Representative illustration of alterations, observed in the cytoplasm of paranodal myelin loops (*arrow*). These changes may correspond to the adaxonal clear spaces illustrated in Fig. 5. *Bars* **A** 10 μm; **B**,**C** 1 μm

Table 2 Nerve morphometry and electrophysiological findings. Teased fiber grading categories: *A/B* normal, *C* paranodal demyelination, *D* segmental demyelination, *E* Wallerian degeneration, *F* segmental remyelination; (*G/ratio* axon diameter/fiber diameter, *CV* conduction velocity, *CMAP* compound muscle action potential, *NA* not available, *nr* non-recordable)

Family	Sex	Age at bx. (years)	Density (mm^2) myelin. fibers sensory/ motor n.	mean G/ratio	Density (mm^2) unmyelin. fibers	Teased fiber study (%)					motor/sensory CV (m/s)			CMAP (mV)	
						A/B	C	D	E	F	median	peroneal	sural	median	peroneal
I[a]	M	16	6,862	0.7±0.07	39,000	61	18	2	3	16	N/A	28.7	nr	N/A	0.3
I[a]	M	61	6,412	0.6±0.09	21,000	77	11	5	2	7	35.1	nr	nr	0.2	nr
V	M	26	8,042	0.55±0.2	49,500	77	14	2	4	3	32.0	35.4	nr	0.3	0.8
VI	M	13	7,042	0.54±0.1	N/A	62	32	0	3	3	32.2	25.8	nr	3.6	0.2
IX	M	45	5,925	0.7±0.09	N/A	66	10	10	2	11	34.8	nr	nr	0.2	nr
X	F	32	N/A	0.65±0.1	N/A	–	–	–	–	–	34.9	29.2	nr	2.7	0.3
XII	M	66	2,250[b]		24,475	41	41	13	2	3	nr	nr	nr	nr	nr
			8,625	0.62±0.11	35,800	38	39	10	4	9					
XIII	F	38	N/A	0.61±0.11	N/A	–	–	–	–	–	35	35	nr	8.2	0.25
XIV	F	50	5,025	0.76±0.06	N/A	–	–	–	–	–	N/A	26	nr	N/A	1.0
XV	F	37	3,609	N/A	N/A	–	–	–	–	–	N/A	31.8	N/A	N/A	0.11
XVI	F	32	6,925	0.7±0.06	N/A	71	24	3	2	0	nr	nr	nr	nr	nr
XVII[a]	F	71	3,062	0.7±0.13	N/A	–	–	–	–	–	32.0	19	nr	8.4	3.6
XVIII	M	14	7,190	0.65±0.08	N/A	46	40	5	2	7	37.5	43.1	37.9	4.8	4.5
C	M	27	9,305	0.52± 0.1	29,000	92	1	1	0	6	50.0	49.0	47.0	11.0	8.0

[a]Findings from Family I and Family XVII have been previously reported [16, 41]
[b]Indicates motor nerve

strated a corresponding progressive loss of motor and sensory axons, confirmed also in morphometric analyses of biopsied motor and sensory nerves [16, 17, 35, 38]. Moreover, in this report we illustrate, in the nerve biopsy of a severely affected young boy, the prominent axonal cytoskeletal changes, which likely precede the actual loss of nerve fibers, observed in later stages of the disease.

Cx 32 gap junction protein is not known to be expressed in nerve axons and at present we have only limited knowledge of its functional role in Schwann cells and in the cell-cell interactions between axons and Schwann cells [7]. However, from the results of recent research it has become increasingly evident that axons and Schwann cells of myelinated nerve fibers form a mutually interdependent unit [13]. It has been shown that molecular defects in myelin genes [PMP22, myelin-associated glycoprotein (MAG), myelin proteolipid protein (PLP)] not only affect myelin stability, but also induce alterations in the axonal cytoskeleton: namely, a reduction in neurofilament phosphorylation, an increase in neurofilament packing density, and a reduction in slow axonal transport and in axonal caliber; altogether these changes lead eventually to a distal axonal degeneration [8, 14, 20, 43]. With this in mind, Sahenk and Chen [34] examined the effect of Schwann cells bearing a mutated Cx 32 protein on axonal cytoskeleton by grafting them into the sciatic nerves of nude mice. With meticulous examination of the nerve xenograft at serial time points for up to 16 weeks, they were able to demonstrate that the *Cx 32* mutation caused profound alterations in the axonal cytoskeleton, characterized by an increase in density of neurofilaments, a depletion in microtubules and an associated fragmentation of smooth endoplasmic reticulum. Axonal atrophy, degeneration and fiber loss were noted in the distal graft segments. These observations indicate that molecular abnormalities of intrinsic Schwann cell proteins can result in profound axonal pathology and in distal accentuated axonal degeneration and fiber loss. Such conclusions are also supported by observations made in mice homozygously deficient of MPZ and considered to represent an appropriate animal model for CMT IB. Longitudinal studies of such animals combined with morphometric analyses demonstrated a progressive loss of motor and sensory axons, occurring clearly in a length-related fashion [10]. The observations are also in agreement with findings in nerve biopsy specimens from children and young adults with dominantly inherited CMT I. Morphometric analyses demonstrated the progressive loss of axons, occurring again in the context of a mutant Schwann cell protein [11]. The mechanisms by which such axonal alterations arise remain to be determined.

Despite the obvious nerve fiber loss, investigation of CMTX biopsy specimens demonstrated unusually prominent signs of axonal regeneration that obviously was not successful. Regenerative clusters of thinly myelinated fibers were frequent, contributing to the observed shift in the myelinated fiber histograms towards smaller fibers [16, 38]. Observed proliferative responses were particularly prominent in the cutaneous sensory nerve of the patient bearing a deletion of the entire coding sequence of the *Cx 32* gene, predictably leading to the absence of Cx 32 protein. Connexins have been implicated in the regulation of cell growth and such regulatory mechanisms may be perturbed in loss-of-function mutations [40].

A further unusual finding concerned abnormalities in the adaxonal and innermost Schwann cell cytoplasm observed by electron microscopy. These included not only complex arrangements of the inner mesaxons, but also a frequent widening of the adaxonal spaces. The latter could even be recognized by light microscopy as adaxonal clear spaces. On ultrastructural examination these spaces were, at times, filled with vesicular material, and such changes appeared to be particularly prominent in paranodal regions. At present, the significance and cause of these alterations is a matter of speculation. One of the putative Cx 32 gap junction functions is the provision of spatial buffering of extracellular potassium that accumulates during axonal excitation [30]. Loss-of-function mutations predictably would compromise such a Schwann cell property. A previous report emphasized pathological alterations at the axo-glial attachment zone, describing transverse band-like structures between decompacted innermost myelin lamellae and the axolemma [39]. Such changes were not noted in our material. However, the paranodes and the axo-glial junctions appeared to be a frequent site of remodeling. Interestingly, similar changes have been found in the adaxonal Schwann cell cytoplasm in the pathology of *Cx 32*-null mice [37].

To elucidate the pathogenesis of CMTX, the consequences of loss of Cx 32 function were studied in *Cx 32*-null mice that were produced by a targeted disruption of the *Cx 32* gene [2, 24, 37]. In careful longitudinal study, Scherer et al. [37] showed that animals lacking the Cx 32 gap junction protein develop a progressive peripheral neuropathy with predominant demyelinative features. Although animals were followed for up to 1 year, axonal changes were not emphasized. However, morphometric analyses had not been not carried out. Heterozygous female animals had milder and non-uniform demyelination, presumably due to the effects of lyonisation occurring randomly in single Schwann cells [22]. From this study, it was concluded that loss of Cx 32 function resulted in a primary Schwann cell defect.

Based on current knowledge, it is likely that mutations in *Cx 32* that lead to loss of function will create a profound perturbation of the Schwann cell-axon unit with resulting pathology in both myelin and axons. The functional consequences of individual *Cx 32* mutations have been studied by testing their ability to form gap junctional channels in the paired *Xenopus* oocyte expression system [32], or by assessing the channel properties in transfected mammalian cells [28, 29, 44]. A proportion of the tested missense mutations were shown not to form functional channels, whereas others retained functional competence, albeit with altered electrophysiological and permeability properties. Therefore, the physiopathological alterations observed in individuals or in families may show some variations. However, it does not seem warranted to distinguish between axonal and demyelinating variant forms of CMTX.

Acknowledgements The authors wish to thank the patients for their participation in this study; Dr. T. Kutzner for his collaboration; Ms. L. Wilkie, Mr. J. A. Stuart, Mr. P. Sindou and Ms. L. Richard for expert technical assistance; and Ms. B. Toth for secretarial assistance. The study was supported by the Research Fund of the London Health Science Centre. Dr. A. F. Hahn held the 1999 Detweiler Travel Fellowship of the Royal College of Physicians and Surgeons of Canada.

References

1. Ainsworth PJ, Bolton CF, Murphy BC, Stuart JA, Hahn AF (1998) Genotype/phenotype correlation in affected individuals of a family with a deletion of the entire coding sequence of the connexin 32 gene. Hum Genet 103: 242–244
2. Anzini P, Neuberg DHH, Schachner M, Nelles E, Willecke K, Zielasek J, Toyka KV, Suter U, Martini R (1997) Structural abnormalities and deficient maintenance of peripheral nerve myelin in mice lacking the gap junction protein connexin 32. J Neurosci 17: 4545–4551
3. Balice-Gordon RJ, Bone, LJ, Scherer SS (1998) Functional gap junctions in the Schwann cell myelin sheath. J Cell Biol 142: 1095–1104
4. Bergoffen J, Scherer SS. Wang S, Oronzi-Scott M, Bone L, Paul DL, Chen K, Lensch MW, Chance P, Fishbeck K (1993) Connexin mutations in X-linked Charcot-Marie-Tooth disease. Science 262: 2039–2042
5. Birouk N, Le Guern E, Maisonabe T, Rouger H, Gouider R, Gugenheim M, Tardieu S, Gugenheim M, Routon MC, Leger JM, Agid Y, Brice A, Bouche P (1998) X-linked Charcot-Marie-Tooth disease with connexin 32 mutations – clinical and electrophysiological study. Neurology 50: 1074–1082
6. Boerkoel CF, Inoue K, Reiter LT, Warner LE, Lupski JR (1999) Molecular mechanisms for CMT1A duplication and HNPP deletion. Ann NY Acad Sci 883: 22–35
7. Bruzzone RC, Ressot C (1997) Connexin, gap junctions, and cell-cell signaling in the nervous system. Eur J Neurosci 9: 1–6
8. De Waegh SM, Lee VM-Y, Brady ST (1992) Local modulation of neurofilament phosphorylation, axonal caliber, and slow axonal transport by myelinating Schwann cells. Cell 68: 451–463
9. Dyck PJ, Karnes J, Lais A, Lofgren EP, Stevens JC (1984) Pathologic alterations of the peripheral nervous system of humans. In: Dyck PJ, Thomas PK, Lambert EH and Bunge R (eds) Peripheral neuropathy, 2nd edn. Saunders, Philadelphia, pp 760–777
10. Frei R, Motzing S, Kinkelin I, Schachner M, Koltzenburg M, Martini R (1999) Loss of distal axons and sensory Merkel cells and features indicative of muscle denervation in hindlimbs of P_0-deficient mice. J Neurosci 19: 6058–6067
11. Gabreels-Festen AAWM, Joosten EMG, Gabreels FJM, Jennekens FGI, Janssen-van Kempen TW (1992) Early morphological features in dominantly inherited demyelinating motor and sensory neuropathy (HMSN type I). J Neurol Sci 107: 145–154
12. Garcia CA (1999) A clinical review of Charcot-Marie-Tooth. Ann NY Acad Sci 883: 69–76
13. Griffin JW, Sheikh K (1999) Schwann cell-axon interactions in Charcot-Marie-Tooth disease. Ann NY Acad Sci 883: 77–90
14. Griffiths I, Klugmann M, Anderson T, Yool D, Thomson C, Schwab MH, Schneider A, Zimmerman F, McCulloch M, Nadon N, Nave K-A (1998) Axonal swellings and degeneration in mice lacking the major proteolipid of myelin. Science 280: 1619–1623
15. Gutierrez A, England JD, Sumner AJ, Ferer S, Warner LE, Lupski JR, Garcia CA (2000) Unusual electrophysiological findings in x-linked dominant Charcot-Marie-Tooth disease. Muscle Nerve 23: 182–188
16. Hahn AF, Brown WF, Koopman WJ, Feasby TE (1990) X-linked dominant hereditary motor and sensory neuropathy. Brain 113: 1511–1525
17. Hahn AF, Bolton CF, White CM, Brown WF, Tuuha SE, Tan CC, Ainsworth PJ (1999) Genotype/phenotype correlations in x-linked dominant Charcot-Marie-Tooth disease. Ann NY Acad Sci 883: 366–382

18. Harding AE (1995) From the syndrome of Charcot, Marie and Tooth to disorders of peripheral myelin proteins. Brain 118: 809–818
19. Ionasescu VV, Searby C, Ionasescu R, Neuhaus IM, Werner R (1996) Mutations of noncoding region of the connexin 32 gene in X-linked dominant Charcot-Marie-Tooth neuropathy. Neurology 47: 541–544
20. Kirkpatrick LL, Brady ST (1994) Modulation of the axonal microtubule cytoskeleton by myelinating Schwann cells. J Neurosci 14: 7440–7450
21. Latour P, Levy N, Paret M, Chapon F, Chazot G, Clavelou P, Couratier P, Dumas R, Allagnon E, Pouget J, Setiey A, Vallat JM, Boucherat M, Vandenberghe A (1997) Mutations in the X-linked form of Charcot-Marie-Tooth disease in the French population. Neurogenetics 1: 117–123
22. Lyon MF (1961) Gene action in the X-chromosome of the mouse. Nature 9: 372–373
23. Mostacciuolo ML, Muller E, Fardin P, Micaglio GF, Bardoni B, Guioli S, Camerino G, Danieli GA (1991) X-linked Charcot-Marie-Tooth disease. A linkage study in a large family by using 12 probes of the pericentromeric region. Hum Genet 87: 23–27
24. Nelles E, Buetzler C, Jung D, Temme A, Gabriel HD, Dahl U, Traub O, Stuempel F, Jungermann K, Zielasek J, Toyka KV, Dermietzel R, Willecke K (1996) Defective propagation of signals generated by sympathetic nerve stimulation in the liver of connexin32-deficient mice. Proc Natl Acad Sci USA 93: 9565–9570
25. Nelis E, Haites N, Van Broeckhoven C (1999) Mutations in the peripheral myelin genes and associated genes in inherited peripheral neuropathies. Hum Mut 13: 11–28
26. Nelis E, Timmerman V, De Jonghe P, Van Broeckhoven C, Rautenstrauss B (1999) Molecular genetics and biology of inherited peripheral neuropathies: a fast-moving field. Neurogenetics 2: 137–148
27. Nicholson G, Nash J (1993) Intermediate nerve conduction velocities define x-linked Charcot-Marie-Tooth neuropathy families. Neurology 43: 2558–2564
28. Oh S, Ri Y, Bennett MVL, Trexler EB, Verselis VK, Bargiello TA (1997) Changes in permeability caused by connexin 32 mutations underlie X-linked Charcot-Marie-Tooth disease. Neuron 19: 927–938
29. Omori Y, Mesnil M, Yamasaki H (1996) Connexin 32 mutations from X-linked Charcot-Marie-Tooth disease patients: functional defects and dominant negative effects. Mol Biol Cell 7: 907–916
30. Orkand PM, Nicholls JG, Kuffler SW (1966) Effect of nerve impulses on the membrane potential of glial cells in the central nervous system of amphibia. J Neurophysiol 29: 788–806
31. Ouvrier R (1996) Correlation between the histopathologic, genotypic, and pheno-typic features of hereditary peripheral neuropathies in childhood. J Child Neurol 11: 133–146
32. Ressot C, Gomes D, Dautigny A, Pham-Dinh D, Bruzzone R (1998) Connexin 32 mutations associated with X-linked Charcot-Marie-Tooth disease show two distinct behaviors: loss of function and altered gating properties. J Neurosci 18: 4063–4075
33. Rozear MP, Pericak-Vance MA, Fischbeck K. Stajich JM, Gaskell PC, Krendel DA, Graham DG, Dawson DV, Roses AH (1987) Hereditary motor and sensory neuropathy, X-linked: a half century follow-up. Neurology 37: 1460–1465
34. Sahenk Z, Chen L (1998) Abnormalities in the axonal cytoskeleton induced by a connexin32 mutation in nerve xenografts. J Neurosci Res 51: 174–184
35. Sander S, Nicholson GA, Ouvrier RA, McLeod JG, Pollard JD (1998) Charcot-Marie-Tooth disease: histopathological features of the peripheral myelin protein (PMP22) duplication (CMT1A) and connexin 32 (CMTX1). Muscle Nerve 21: 217–225
36. Scherer SS, Deschenes SM, Xu Y-T, Grinspan JB, Fischbeck KH, Paul DL (1995) Connexin 32 is a myelin-related protein in the PNS and CNS. J Neurosci 15: 8281–8294
37. Scherer SS, Xu Y-T, Nelles E, Fischbeck K, Willecke K, Bone LJ (1998) Connexin 32-null mice develop a demyelinating peripheral neuropathy. Glia 24: 8–20
38. Senderek J, Bergmann C, Quasthoff S, Ramaekers VT, Schroder JM (1998) X-linked dominant Charcot-Marie-Tooth disease: nerve biopsies allow morphological evaluation and detection of connexin32 mutations (Arg15Trp, Arg22Gln). Acta Neuropathol 95: 443–449
39. Senderek J, Hermanns B, Bergmann C, Boroojerdi B, Bajbouj M, Hungs M, Ramaekers VT, Quasthoff S, Karch D, Schroder JM (1999) X-linked dominant Charcot-Marie-Tooth neuropathy: clinical, electrophysiological, and morphological phenotype in four families with different connexin32 mutations. J Neurol Sci 167: 90–101
40. Suter U, Snipes GJ (1995) Biology and genetics of hereditary motor and sensory neuropathies. Annu Rev Neurosci 18: 45–75
41. Tabaraud F, Lagrange E, Sindou P, Vandenberghe A, Levy N, Vallat JM (1999) Demyelinating x-linked Charcot-Marie-Tooth disease: unusual electrophysiological findings. Muscle Nerve 22: 1442–1447
42. Thomas PK, Marques W, Davis MB, Sweeney MG, King RHM, Bradley JL, Muddle JR, Tyson J, Malcom S, Harding AE (1997) The phenotypic manifestations of chromosome 17p11.2 duplication. Brain 120: 465–478
43. Yin X, Crawford TO, Griffin JW, Tu P, Lee VM-Y, Li C, Roder J, Trapp BD (1998) Myelin-associated glycoprotein is a myelin signal that modulates the caliber of myelinated axons. J Neurosci 18: 1953–1962
44. Yoshimura T, Satake M, Ohnishi A, Tsutsumi Y, Fujikura Y(1998) Mutations of connexin32 in Charcot-Marie-Tooth disease Type X interfere with cell-to-cell communication but not cell proliferation and myelin-specific gene expression. J Neurosci Res 51: 154–161